

Ultimately, the compatibility of the OCE data analysis with sea truth will have to be tested when buoy measurements and wind field data for 14 November 1981 become available. However, historical current measurements show a strong surface current in the upper 100 m near the entrance to the strait. This current flows into the Mediterranean along the coasts of North Africa and Spain. Also, a relatively saline Mediterranean under-current flows out from the strait at below 100 m and surfaces some distance into the Atlantic.

**Bathymetry.** The Great Bahama Bank forms a semicircular shoal whose depth ranges from few meters to tens of meters. Gradients in depth occur at the northern edges, known as the Tongue of the Ocean. This topographic feature is surrounded with seawater of low oxygenation. Thus, the area is characterized by a scarcity of planktonic marine life. These conditions make the area highly suitable for visual observation of the underwater topography. The blue-green components of visible light, in the absence of chlorophyll pigment, penetrate deep into the water and reflect from the bottom. Data obtained at 0824 hours (EST) during orbit 32, in the vicinity of Nassau and Andros Island, were processed to depict underwater topographic features of the Great Bahama Bank (Fig. 7). The enhanced false-color image is based on the upwelling radiance of the band at 518 nm. The return signal is related inversely to the depth of the water. Upwelling spectral radiances taken from a shallow zone and from a deepwater zone represented in Fig. 7 are shown in Fig. 8. The dotted lines (sub-surface radiance) are corrected for the atmospheric effects; hatched areas represent bottom reflection signals.

**Discussion.** Because of the orbiter's shortened mission, the OCE netted only a minimum amount of data for clear ocean views. Also, some of the surface experiments that were designed to validate interpretations of OCE observations were not carried out because of the rescheduling of the shuttle launch date. In spite of these difficulties, we believe that the primary objectives of the OCE were achieved. A wide variety of phenomena were observed and analyzed from the color expressions of the ocean.

The OCE demonstrated that, properly treated, ocean colorimetry provides a simple and direct method of remotely sensing the oceans. Until now, oceanographic studies incorporating satellite imagery of visible color have been limited to inferring near-shore and estuarine circulation. In those regimes high reflec-

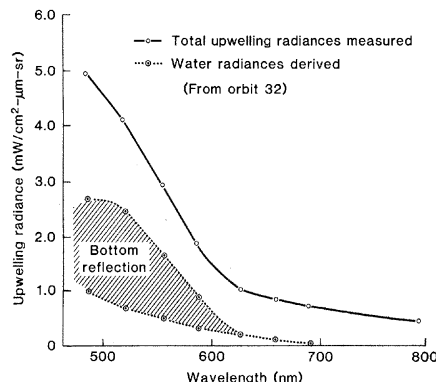


Fig. 8. Spectral curves for two selected areas of the scene in Fig. 7, showing total upwelling radiance from a shallow zone of the Great Bahama Bank as perceived by the sensor (solid line) and the derived water radiance (upper dotted line). The derived water radiance from an area of deep water, the Tongue of the Ocean, is shown by the lower dotted line.

tivity of suspended material provides a relatively easily identified signature. The method of detecting variations in chlorophyll concentration in spatial and temporal domains promises to provide a new dimension.

To measure the concentrations of phytoplankton pigments in the ocean, the radiance detected at satellite altitudes needs to be corrected for atmospheric effects. The method devised to remove aerosol effects for the CZCS is a possible alternative (6). But in our OCE analysis a sophisticated model was incorporated to account for all the components in absolute radiance (Table 2). The outcome of such a method provides us with a consistent relation between the signal mea-

sured and the concentration of the chlorophyll pigments in the open ocean (7). However, the spectral curves in Figs. 3 and 8 imply that chlorophyll analyses are still limited to oceanic conditions of hydrospheric homogeneity and clarity.

The method of using chlorophyll concentration as a tracer may be applied to the deduction of oceanic flow patterns in large areas (Fig. 6). Plankton patches are natural drifters and can be tracked by satellites. Thus the color scanner has proved its utility in studies of both ocean circulation and biological processes.

HONGSUK H. KIM

NASA/Goddard Space Flight Center,  
Greenbelt, Maryland 20771

WILLIAM D. HART

Science Systems and Applications,  
Inc., Seabrook, Maryland 20801

HEINZ VAN DER PIEPEN

Deutsche Forschungs und  
Versuchsanstalt für Luft und  
Raumfahrt, 8031 Wesseling,  
Federal Republic of Germany

#### References and Notes

1. G. L. Clarke, G. C. Ewing, C. J. Lorenzen, *Science* **167**, 1119 (1970).
2. H. H. Kim, C. R. McClain, L. R. Blaine, W. D. Hart, L. P. Atkinson, J. A. Yoder, *J. Geophys. Res.* **85**, 3982 (1980); H. H. Kim, C. R. McClain, W. D. Hart, *ibid.* **86**, 6669 (1981).
3. W. A. Hovis *et al.*, *Science* **210**, 60 (1980).
4. J. V. Dave, "Development of programs for computing characteristics of ultraviolet radiation" (Tech. Rep. SPA-D, NASA contract NAS5-2168, IBM, Palo Alto, Calif., 1972).
5. R. V. Legeckis, *J. Phys. Oceanogr.* **9**, 483 (1979).
6. H. Gordon, *Appl. Opt.* **17**, 1631 (1978).
7. J. A. Yoder, L. P. Atkinson, T. N. Lee, H. H. Kim, C. R. McClain, *Limnol. Oceanogr.* **26**, 1103 (1981).
8. D. Clem and B. Johnson were responsible for the flawless performance of the OCE instrument during the shuttle mission.

20 August 1982

## Feature Identification and Location Experiment

**Abstract.** The feature identification and location experiment (FILE) senses radiation from the earth in spectral bands centered at 0.65 and 0.85 micrometers and compares ratios of the reflected solar radiation in the two wavelengths to make real-time classification decisions about four primary features: water, vegetation, bare land, and a cloud-snow-ice class. The radiance ratio classification algorithm successfully made automatic data-selection decisions. The classification image obtained on the mission is providing information needed to evaluate the FILE algorithm and system performance.

The feature identification and location experiment (FILE) (Fig. 1) was flown on the second space shuttle flight to test a technique for real-time autonomous classification of four primary earth features—water; vegetation; bare land; and clouds, snow, and ice. The experiment, based on a simple and easily implemented classification algorithm, is considered a logical step toward providing the advanced technology needed to achieve

data selectivity at the sensing stage, thus reducing the data load and delays in the data handling and data dissemination in earth monitoring and data-gathering missions. This classification technique is contributing to the development of advanced cloud detection, pointing, tracking, and navigation technology.

A FILE development instrument was first flown in aircraft, and about 1500 images were obtained in cross-country

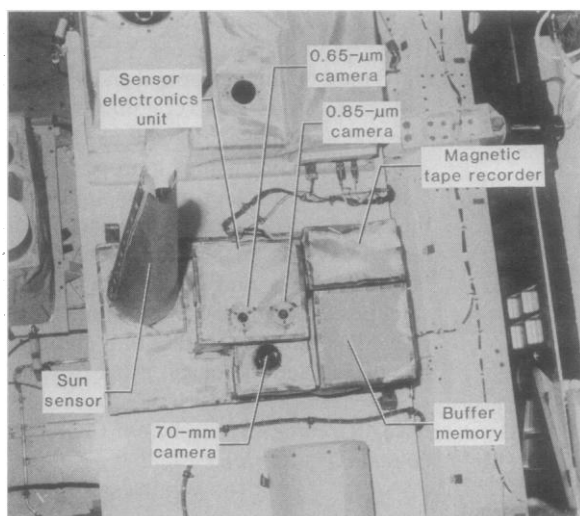


Fig. 1. FILE assembly for the shuttle scientific payload.

flights and flights over the west and east coasts of the United States before the spacecraft instrument was flown on the shuttle.

The FILE senses earth radiation in two spectral bands, centered at 0.65 and 0.85  $\mu\text{m}$ , with a 0.02- $\mu\text{m}$  bandwidth. Ratios from the sensed spectral radiance data (solar power reflected from the features) are used (1-4) to classify features. In relative terms, green vegetation has a low reflectance at 0.65  $\mu\text{m}$ , due to the chlorophyll absorption band, and a higher reflectance at 0.85  $\mu\text{m}$ . Water has a high reflectance at 0.65  $\mu\text{m}$  and a lower reflectance at 0.85  $\mu\text{m}$ . Therefore, water and vegetation can be clearly distinguished from the ratio of the 0.65- $\mu\text{m}$  camera signal to the 0.85- $\mu\text{m}$  camera signal (Fig. 2). The bare land ratio lies between the ratios for vegetation and water. The cloud-snow-ice class gives camera signal ratios that are not distinct from those for water and bare land but are greater than those for vegetation, and this class will have a 0.65- $\mu\text{m}$  camera signal output exceeding that for either water or bare land. Therefore, with some knowledge of the angle of the sun, a 0.65- $\mu\text{m}$  radiance threshold can be established to distinguish either bare land or water from clouds, snow, and ice.

It should be emphasized that feature classification by FILE, as a function of the 0.65- and 0.85- $\mu\text{m}$  camera signals, is approximate, consistent with a simple experimental algorithm (Fig. 2), the boundaries of which divide the camera-signal space into areas that have a high probability of representing the corresponding earth features. A number of variables and their ranges are taken into consideration to derive the classification boundaries (3, 4). The variables include atmospheric visibility, solar zenith an-

gle, solar sensor azimuthal angle, and sensor viewing angle. For the derivations in this experiment, it is assumed that the flight  $\beta$  angle is small, that is, that the line between the earth and the sun is within a few degrees of the orbit plane. Evaluation of the accuracy of the boundary approximation algorithm (Fig. 2) is a primary objective of obtaining and processing the FILE data. The FILE records spectral radiance data that may be processed after the flight for classification algorithm modification, evaluation, and optimization.

The FILE experiment has five subassemblies (Fig. 3): a sunrise detector, a

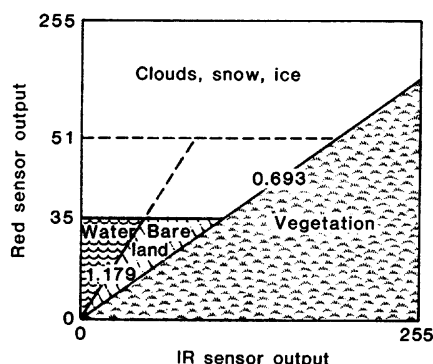


Fig. 2. FILE algorithm.

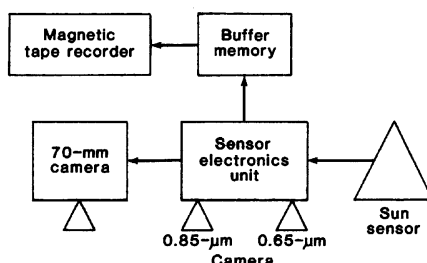


Fig. 3. The major FILE components.

sensor electronics unit with the two charge-coupled devices (CCD) cameras and associated camera electronics, a buffer memory storage unit, a magnetic tape recorder, and a 70-mm film camera. The sunrise detector initializes (sets to a starting point) a timer in the electronics unit that controls the experiment and data-taking sequence; FILE was programmed to collect and classify 19 images per orbit. The buffer memory package stores the digital data from the electronics unit and transfers them to the tape recorder at a compatible data rate. The tape recorder has a storage capacity for 120 frames of data. The film camera, which is boresighted with the CCD cameras, has film storage for 120 images. The CCD camera resolution is 1 km by 0.75 km, and the field of view is 17° by 23°. The photographic camera field of view is 29° by 29°.

Real-time classification decisions are made by the instrument and are based on the FILE algorithm (Fig. 2). Radiance ratios and the 0.65- $\mu\text{m}$  camera output are compared electronically with decision thresholds, and the comparator outputs are logically combined to provide the feature classifications. For each image the classification decision is made individually for each camera pixel (10,000 pixels, 100 by 100 CCD array elements), and the number of pixels classified into each feature category, as well as the individual pixel signal level for each camera, is recorded on magnetic tape. For each image, Greenwich mean time is recorded and a color photograph is taken.

In addition to recording images, FILE evaluates each image and flags those that contain 80 percent or more of a given feature (water, clouds, or bare earth). Flagged images are counted, and the count is used to selectively inhibit recording certain image classes. This autonomous decision-making capability allows a well-distributed sample of scenes to be collected during a mission.

The experiment was activated for 38 hours of the total 54-hour mission time, and photographic images (70 mm) were recorded (87-second data-taking intervals) during orbits 8, 9, 10, and 11 of the mission (12 through 14 November 1981). The orbit was circular at 138 nautical miles, with a period of 1 hour, 29 minutes, and 40 seconds.

Although FILE was designed to operate with low  $\beta$  angles, launch delays and mission changes resulted in excessively high  $\beta$  angles throughout the mission, limiting data-taking opportunities. High  $\beta$  angles resulted in low sun angles (max-

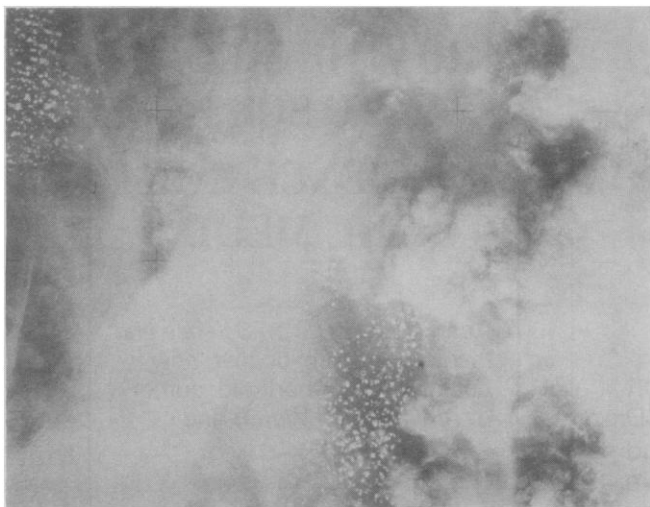


Fig. 4 (left). FILE photographic image of cloud cover (light areas) over ocean (dark areas). Features in Fig. 4.

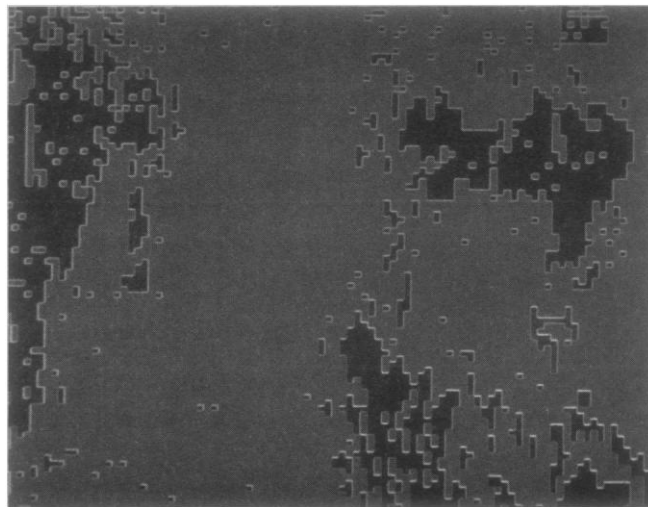


Fig. 5 (right). FILE classification image of the features in Fig. 4.

imum sun angle =  $90 - \beta$ ) and accompanying low amplitude signals within the 0.65- and 0.85- $\mu\text{m}$  bands. Of the 44 photographic images collected, 25 were nadir looking and 19 were either oriented toward deep space or the dark side of the earth, because of an unscheduled adjustment maneuver of the shuttle's inertial measurement unit. Solid-state camera data (magnetic tape) were recorded only for the first of the nadir-looking images made during orbit 8.

The first image (Fig. 4) contains a complex mixture of cloud cover over ocean. Inappropriate tape recorder preflight initialization precluded the recording of additional solid-state camera images. Postflight review and analysis indicate that at least two factors may have contributed to this anomaly: recorder design that precluded verification of initial tape position, and the influence on tape initialization of the shutdown sequence of the power supplies for the tape recorder ground support equipment. Although additional solid-state camera image data were not recorded, 70-mm FILE photographs, mission operations data, and photographic sequences from other experiments provided a data base for evaluating overall performance of the FILE system and its components. The image recorded (Fig. 4) contained pixel data for 57 percent of the image. Fifty lines (every other line) were recorded for the full-frame field of view, and seven additional lines (interlaced from the top edge of the frame) were recorded.

Pixels composing the CCD camera-recorded images were processed digitally postflight to generate average pixel values. These values were assigned for the missing pixels and were used to

generate reconstructed images for the 0.65- and 0.85- $\mu\text{m}$  CCD data. Since large continuous areas of clouds and water are present in the image (Fig. 4), this pixel averaging technique does not introduce significant errors. The FILE algorithm was used to reconstruct images for the 0.65- and 0.85- $\mu\text{m}$  cameras and to obtain the composite classification image (Fig. 5). This classification image clearly identifies the major openings within the cloud structure where the underlying ocean areas have been properly classified as water.

In the FILE processing, different pixel colors are assigned for water, vegetation, bare earth, and the cloud-snow-ice class (blue, green, yellow, and white, respectively). In Fig. 5, 7383 pixels are classified as bare earth. Evaluation of Fig. 4 indicates that most of this area is cloud cover. Two factors contributed to this misclassification: (i) the low sun angle ( $< 40^\circ$ ) that existed when the data were recorded (ii) and lower than anticipated 0.65- $\mu\text{m}$  camera signal level. These reduced signal levels result in radiance ratio values that fall primarily within the water and bare earth classification triangles, below the cloud level threshold (Fig. 2).

To evaluate this low-signal-level misclassification, first, the cloud threshold level was lowered. A threshold of 20 (0.65- $\mu\text{m}$  camera) (Fig. 2) was found to significantly improve cloud classification. Second, analysis of the data, based on an assumed flat spectral response for clouds, indicated that a gain of 2.5 should be applied to the 0.65- $\mu\text{m}$  camera signal; this also improved cloud classification.

Study of the limited FILE photograph-

ic data in parallel with photographic and mission data from other experiments indicates that FILE functioned, as designed, to automatically make data-selection decisions. The classification image obtained is providing data needed to evaluate processing, algorithm, and system performance. Together with data collected from aircraft flights, the FILE shuttle experiment results indicate that radiance ratio technology has strong potential for use in the development of advanced classification decision-making systems for onboard, real-time applications. Additional space flight data should be available in 1984 after FILE is flown as part of the scientific payload scheduled for launch on a 1984 shuttle flight. In addition, an advanced four-channel instrument is being tested on aircraft flights.

W. E. SIVERTSON, JR.

R. GALE WILSON

GORDON F. BULLOCK

NASA Langley Research Center,  
Hampton, Virginia 23665

R. T. SCHAPPELL  
Martin Marietta, Denver Aerospace  
Division, Denver, Colorado 80201

#### References and Notes

1. R. G. Wilson et al., *Proceedings of the IEEE Computer Society Conference on Pattern Recognition and Image Processing* (IEEE, New York, 1979), pp. 623-629.
2. W. E. Sivertson and R. G. Wilson, in *Optical Pattern Recognition*, D. Casasent, Ed. (Society of Photo-Optical Instrumentation Engineers, Washington, D.C., 1979), vol. 201, pp. 17-26.
3. R. T. Schappell, J. C. Tietz, H. M. Thomas, J. W. Lowrie, *NASA Contract Rep. CR-158997* (February 1979).
4. R. T. Schappell, J. C. Tietz, R. L. Hulstrom, R. A. Cunningham, *ibid. CR-145-122* (December 1976).
5. FILE is a joint effort of the NASA Langley Research Center and Martin Marietta, under contract to NASA.

20 August 1982